The Journal of Engineering

Research Article

IET Journals
The Institution of Engineering and Technology

Modelling and simulation of a smartgrid architecture for a real distribution network in the UK

eISSN 2051-3305
Received on 1st July 2019
Accepted on 4th July 2019
E-First on 17th July 2019
doi: 10.1049/joe.2018.8217
www.ietdl.org

Jialiang Yi[1], Chloe Pages[2], Adib Allahham[1] ✉, Damian Giaouris[1], Charalampos Patsios[1]

[1]*Urban Science Building, Newcastle University, Newcastle upon Tyne, NE4 5TG, UK*
[2]*St Microelectronics Crolles 300, 850 rue Jean Mommet, 38920 Crolles, France*
✉ *E-mail: adib.allahham@ncl.ac.uk*

Abstract: As part of the inteGRIDy project, funded by the European Commission, an investigation is carried out on a real distribution network, where high penetrations of distributed generations (DGs) exist, in the UK. In this study, a model of this network is built. In this model, additional energy storage systems are located in the network close to DGs to represent future smartgrid architecture. This architecture is proposed to reduce the power import and export between this network and the grid. Four test cases are designed to explore the impacts of DG and the benefits of ESSs.

1 Introduction

At COP 21 Paris December 2015, 195 countries have agreed to limit global temperature rise to below 2°C above pre-industrial levels. The European Union is committed to reduce greenhouse gas emissions by 40% by 2030 and achieve 20% penetration of renewables by 2020. In the United Kingdom, energy supply, transport, business, and residential sectors account for 78% of total UK CO_2 emissions in total in 2013. Transport and residential sectors contribute 20 and 13% of total CO_2 emissions, therefore, decarbonising of transportation, heating and electricity generation is important to realise this target. The anticipated increasing adoption of electrical vehicles, heat pumps and renewable energy sources will bring challenges and opportunities to distribution networks.

The integrated smart GRID cross-functional solutions for optimised synergetic energy distribution, utilisation storage technologies (inteGRIDy) project, an H2020 project funded by the European commission, aims to integrate cutting-edge technologies, solutions, and mechanisms in a scalable cross-functional modular platform (CMP). The CMP will consist of functions of network modelling, prosumer profiling, demand side response (DSR) matching, energy storage system (ESS) control, forecasting, and multi-objective optimisation-based energy management system, and aims to improve the operation of distribution networks with high penetration of distributed generation (DG) and smartgrid interventions.

Ten pilot cases across the EU are being set up to demonstrate a range of smartgrid technologies and techniques including photovoltaic (PV), electric vehicle (EV), thermal storage, ESSs, and DSR. Isle of Wight (IoW), locates in south England, is one of the pilot cases of the project and aims to become self-sufficient in electricity supply. However, due to the increasing penetration of DG, network constraint violations are already likely to occur. To avoid expensive and time consuming network reinforcement, the inteGRIDy project consortium is developing smartgrid architecture for IoW to defer or avoid network reinforcement. Fast EV charging facilities, DSR and ESS will be trialled.

In this study, the electrical network of IoW is introduced. The steady-state electrical network model has been built and integrated into a test environment for smartgrid technologies and techniques. Simulation results using ESS to increase voltage headroom is given.

2 Method

In this section, the IoW distribution network is introduced. The modelling process of this network in detailed. The deployment of ESSs in the proposed future smartgrid architecture is discussed. In this study, the optimal power flow (OPF) technique is applied to ESS control. The application of OPF in this problem is presented. Finally, how OPF-based ESS control is integrated with an on-load tap changer control scheme is introduced.

2.1 IoW distribution network

The IoW is supplied from the mainland by three subsea interconnectors and distribute power through 132/33 kV primary substations. A 140 MW oil-fired power station provides emergency supplies for the Island and operates primarily as a short-term operating reserve facility. At 33 kV level, a number of DGs including PV and tidal power have been connected or accepted. Distributed PV systems have been installed on over 3,000 domestic and commercial buildings. The increasing reinforcement penetration of DG has triggered the necessary network (Fig. 1).

However, conventional reinforcement is expensive and also has an impact on the environment. The implementation of smartgrid has the potential to avoid or minimise the requirement for network reinforcement and maximise DG output. The proposed smartgrid architecture will include ESSs and DSR. ESS and DSR will be used for minimising the net import/export of the island through the interconnector and also take into consideration power flow and voltage constraints. The use of ESS, DSR, and other smartgrid technologies and techniques can also increase the rating of the DG connected to the distribution network and avoid or delay network reinforcement.

2.2 Modelling of IoW network

The steady-state model 132 and 33 kV network of IoW is modelled in IPSA2 and MATPOWER [1] based on [2]. This model will be used for three purposes. First of all, establish the baseline by running sequential load flow with load and generation profiles for different scenarios. Potential constraints due to the increasing penetration of DG and load will be identified. Secondly, this model will be used to carry out pre-trial simulations to build confidence that the trials will not cause network limit violations. Finally, after the trials, this model will be validated with real data. The validated and improved model will be used to extrapolate new scenarios, simulate unfeasible trials and generalised to explore the benefits of smartgrid and the CMP on other networks. An established methodology using previous UK smartgrid projects is applied [3] in this process.

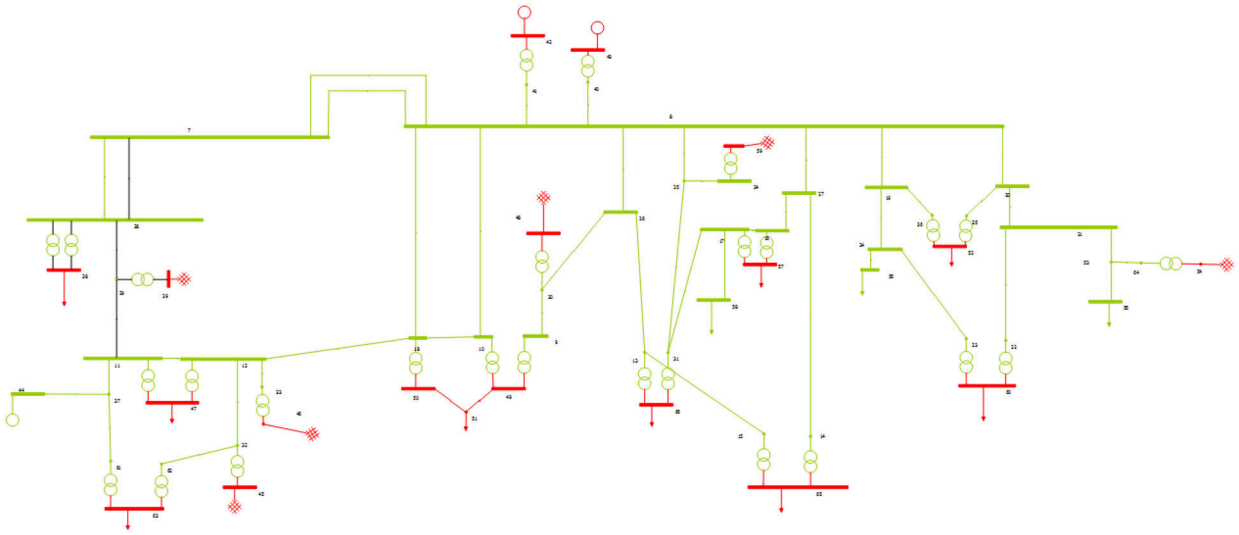

Fig. 1 *HV network model of IoW in IPSA2*

2.3 Energy storage systems (ESSs)

The benefits of grid scale ESS are well studied [4]. A number of applications of ESS in a smartgrid environment can be found. In [5], a multi-objective control strategy for battery energy storage systems (BESS) is proposed to defer network reinforcement due to the increasing penetration of PV. OPF-based ESS control methods have been proposed in [6, 7]. In [6], an ESS is instructed to charge during off-peak periods and discharge during peak periods. Maximum real power import and export is decided by the maximum mismatch between generation and load. In this study, the charge and discharge operation periods are fixed. In [7], the authors proposed a dynamic programming approach-based solver for OPF problems with ESS, with a focus on microgrid application.

2.4 Optimal power flow (OPF)

OPF is a well-established technique for solving power system control and planning problems. In this study, OPF is adopted for ESS control. The generic OPF formulation is modified to minimise the cost of using a conventional generator, maximise DG output and minimise the cost of using ESS. The formulation of the modified OPF is introduced below.

2.4.1 Objective function:

$$f_{(X)} = f_{\mathrm{g}} + f_{\mathrm{DG}} + f_{\mathrm{ESS}} \tag{1}$$

where

$$\boldsymbol{X} = [\boldsymbol{P}_{\mathrm{g}}, \boldsymbol{P}_{\mathrm{DG,Curtailment}}, \boldsymbol{P}_{\mathrm{ESS}}, \boldsymbol{Q}_{\mathrm{g}}, \boldsymbol{Q}_{\mathrm{DG}}, \boldsymbol{Q}_{\mathrm{ESS}}]$$

Equation (1) is detailed with (2)–(4) below

$$f_{\mathrm{g}} = \sum_{i=1}^{N_{\mathrm{g}}} \left[f_{gi,P}(P_{gi}) + f_{gi,Q}(Q_{gi}) \right] \tag{2}$$

$$f_{\mathrm{DG}} = \sum_{i=1}^{N_{\mathrm{DG}}} (C_{\mathrm{DG}_i,\mathrm{Curtailment}} \cdot P_{\mathrm{DG}_i,\mathrm{Curtailment}} + C_{\mathrm{DG}_i,Q} \cdot Q_{\mathrm{DG}_i}) \tag{3}$$

$$f_{\mathrm{ESS}} = \sum_{i=1}^{N_{\mathrm{ESS}}} (|C_{\mathrm{ESS}_i,P} \cdot P_{\mathrm{ESS}_i}| + |C_{\mathrm{ESS}_i,Q} \cdot Q_{\mathrm{ESS}_i}|) \tag{4}$$

where $\boldsymbol{P}_{\mathrm{DG,Curtailment}}$ is the set of real power curtailment of DG; $\boldsymbol{P}_{\mathrm{DG,Max}}$ is the set of maximum real power output of DG; $\boldsymbol{P}_{\mathrm{ESS}}$ is the set of real power import/export of ESS; $\boldsymbol{P}_{\mathrm{G}}$ is the set of generator real power outputs; $\boldsymbol{Q}_{\mathrm{G}}$ is the set of generator reactive power outputs; $\boldsymbol{Q}_{\mathrm{ESS}}$ is the set of reactive power import/export of ESS; $C_{\mathrm{DG}_i,\mathrm{Curtailment}}$ is the cost of real power curtailment of DG i; $C_{\mathrm{DG}_i,Q}$ is the cost of reactive power of DG i; $C_{\mathrm{ESS}_i,\mathrm{P}}$ is the cost of real power of ESS i; $C_{\mathrm{ESS}_i,Q}$ is the cost of reactive power of ESS i.

Equation (2) calculates the total cost of using conventional generators. Equation (3) calculates the cost of DG real power curtailment and the use of reactive power. Equation (4) calculates the cost of using ESS.

2.4.2 Constraints:

$$\boldsymbol{V}_{\mathrm{Min}} \le \boldsymbol{V} \le \boldsymbol{V}_{\mathrm{Max}} \tag{5}$$

$$|\boldsymbol{S}_{\mathrm{Branch,Send}}| \le \boldsymbol{S}_{\mathrm{Branch,Rating}} \tag{6}$$

$$|\boldsymbol{S}_{\mathrm{Branch,Receive}}| \le \boldsymbol{S}_{\mathrm{Branch,Rating}} \tag{7}$$

$$\boldsymbol{P}^{\mathrm{Lower}}_{\mathrm{G,Rating}} \le \boldsymbol{P}_{\mathrm{G}} \le \boldsymbol{P}^{\mathrm{Lower}}_{\mathrm{G,Rating}} \tag{8}$$

$$\boldsymbol{Q}^{\mathrm{Lower}}_{\mathrm{G,Rating}} \le \boldsymbol{Q}_{\mathrm{G}} \le \boldsymbol{Q}^{\mathrm{Upper}}_{\mathrm{G,Rating}} \tag{9}$$

$$0 \le \boldsymbol{P}_{\mathrm{DG,Curtailment}} \le \boldsymbol{P}_{\mathrm{DG,Max}} \tag{10}$$

$$\boldsymbol{Q}^{\mathrm{Lower}}_{\mathrm{DG,Rating}} \le \boldsymbol{Q}_{\mathrm{DG}} \le \boldsymbol{Q}^{\mathrm{Upper}}_{\mathrm{DG,Rating}} \tag{11}$$

$$\boldsymbol{P}^{\mathrm{Lower}}_{\mathrm{ESS,Rating}} \le \boldsymbol{P}_{\mathrm{ESS}} \le \boldsymbol{P}^{\mathrm{Upper}}_{\mathrm{ESS,Rating}} \tag{12}$$

$$\boldsymbol{Q}^{\mathrm{Lower}}_{\mathrm{ESS,Rating}} \le \boldsymbol{Q}_{\mathrm{ESS}} \le \boldsymbol{Q}^{\mathrm{Upper}}_{\mathrm{ESS,Rating}} \tag{13}$$

$$\boldsymbol{S}^{\mathrm{Lower}}_{\mathrm{ESS}} \le \boldsymbol{S}_{\mathrm{ESS}} = \sqrt{\boldsymbol{P}^2_{ESS} + \boldsymbol{Q}^2_{\mathrm{ESS}}} \le \boldsymbol{S}^{\mathrm{Upper}}_{\mathrm{ESS}} \tag{14}$$

$$\begin{aligned} E_{\mathrm{ESS}_i,t=t_0+\Delta t} = {} & E_{\mathrm{ESS}_i,t=t_0} + d_{\mathrm{ESS}_i} \cdot P_{\mathrm{ESS}_i} \cdot \eta_{\mathrm{ESS}_i} \\ & + (1 - d_{\mathrm{ESS}_i}) \cdot \frac{P_{\mathrm{ESS}_i}}{\eta_{\mathrm{ESS}_i}}, \mathrm{ESS}_i \in \Lambda_{\mathrm{ESS}} \end{aligned} \tag{15}$$

$$E^{\mathrm{Lower}}_{\mathrm{ESS}_i} \le E_{\mathrm{ESS}_i,t=t_0+\Delta t} \le E^{\mathrm{Upper}}_{\mathrm{ESS}_i} \tag{16}$$

where $\boldsymbol{V}$ is the set of bus voltage; $\boldsymbol{V}_{\mathrm{Max}}$ is the set of upper limit of bus voltage; $\boldsymbol{V}_{\mathrm{Min}}$ is the set of lower limit of bus voltage; $\boldsymbol{S}_{\mathrm{Branch,Rating}}$ is the set of branch power flow ratings; $\boldsymbol{S}_{\mathrm{Branch,Receive}}$ is the set of branch power flows at the receiving ends; $\boldsymbol{S}_{\mathrm{Branch,send}}$ is the set of branch power flows at the sending ends; $\boldsymbol{P}^{\mathrm{Lower}}_{\mathrm{G,Rating}}$ is the set of generator real power lower ratings; $\boldsymbol{P}^{\mathrm{Upper}}_{\mathrm{G,Rating}}$ is the set of generator real power upper ratings; $\boldsymbol{P}^{\mathrm{Lower}}_{\mathrm{G,Rating}}$ is the set of generator real power upper ratings; $\boldsymbol{Q}^{\mathrm{Upper}}_{\mathrm{G,Rating}}$ is the set of generator reactive

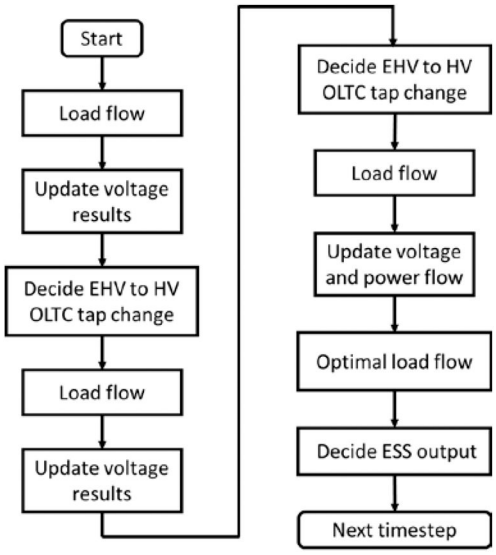

Fig. 2 *Flow chart of the control scheme*

power upper ratings; $\boldsymbol{P}_{\mathrm{DG,Max}}$ is the set of maximum real power output of DG; $\boldsymbol{P}_{\mathrm{ESS}}$ is the set of real power import/export of ESS; $\boldsymbol{P}^{\mathrm{Lower}}_{\mathrm{ESS,Rating}}$ is the set of lower real power limits of ESS; $\boldsymbol{P}^{\mathrm{Upper}}_{\mathrm{ESS,Rating}}$ is the set of upper real power limits of ESS; $\boldsymbol{Q}_{\mathrm{ESS}}$ is the set of reactive power import/export of ESS; $\boldsymbol{Q}^{\mathrm{Lower}}_{\mathrm{ESS,Rating}}$ is the set of lower reactive power limits of ESS; $\boldsymbol{Q}^{\mathrm{Upper}}_{\mathrm{ESS,Rating}}$ is the set of upper reactive power limits of ESS; $\boldsymbol{S}_{\mathrm{ESS}}$ is the set of apparent power import/export of ESS; d_{ESS_i} is the binary charge and discharge sign of ESS i, $d_{\mathrm{ESS}_i} = 1$ if charge and 0 if discharge; ESS_i, t is the energy available in ESS i at time t; $E^{\mathrm{Lower}}_{\mathrm{ESS}_i}$ is the lower limit of energy available in ESS i; $E^{\mathrm{Upper}}_{\mathrm{ESS}_i}$ is the upper limit of energy available in ESS i; and η_{ESS_i} is the efficiency of ESS i.

Constraint (5) ensures all bus voltages are within the limit between 0.94 and 1.06 p.u. Constraints (6) are apparent power rating constraints for sending ends of transformers, cables, and overhead lines. Apparent power rating constraints of receiving ends are introduced in (7). Equations (5)–(7) are network constraints. Constraints (8) and (9) are real and reactive power constraints for conventional generators. Equation (10) defines the lower and upper limits of DG real power curtailment. Lower and upper limits of DG real power output are decided based on the type of DG. For renewable-based DG, maximum DG curtailment is the current DG real power output, i.e. $P_{\mathrm{DG,Max}} = P_{\mathrm{DG}}$ and minimum DG curtailment is 0, which means it is not curtailed. Equation (11) is the reactive power output constraints of DG. Real power, reactive power and apparent power rating limits for ESS are defined by (12)–(14). Energy stored in the ESS system is calculated with (15). In this equation, $P_{\mathrm{ESS}_i} > 0$ means charging and $P_{\mathrm{ESS}_i} < 0$ means discharge. d_{ESS_i} is a binary number to indicate charging or discharging. d_{ESS_i} is 1 if charge and 0 if discharge. Constraint (16) prevents over charge and over discharge of ESS for current and next time step.

2.5 Control methodology

The control method applied in this study is illustrated in Fig. 2. Online tap changers (OTLC) exist at two voltage levels from extra high voltage (EHV) to high voltage (HV) and from HV to medium voltage (MV). MV to low-voltage transformers are not equipped with OLTC. The OLTC control method adopted in this study is consistent with the industrial control scheme. OLTCs from EHV to HV operates first so that the voltage at the secondary side of the transformers are maintained at 1.03. A bandwidth of 0.01875 is applied to avoid frequent OLTC operation. OLTCs from HV to MV operates after upstream OLTCs. The same target voltage and bandwidth are used for HV to MV OLTCs. ESS outputs, decided by OPF techniques, are applied after all OLTC tap changes are confirmed.

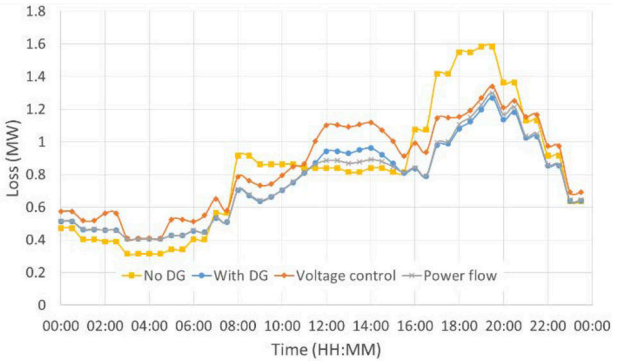

Fig. 3 *Total network losses*

Table 1 Total network losses in 24 h

Test case		Total network losses in 24 h, MWh
1	No DG	19.66
2	With DG	18.02
3	ESS for voltage control	20.31
4	ESS for power management	17.99

3 Simulation results

Four test cases have been evaluated. The first scenario only includes demand but no DG. The second includes both demand and DG. In the third and fourth test cases, five ESSs are located in the networks next to DGs. OPF techniques described earlier are applied in scenario three and four with different objectives. In the third test case, ESSs are used for voltage control. The control objective is to maintain the voltage of all buses between 0.97 and 1.03 p.u. with reactive power only. In the fourth scenario, ESSs are used for power flow management so that reverse power flow from the island to the mainland is avoided. Meanwhile, the voltage limit between 0.97 and 1.03 p.u. is also applied. In this scenario, only real power is used.

The following indices are used to evaluate the effects of DG and ESS: voltage headroom, power flow headroom, number of tap change and network losses. Increasing voltage headroom means higher capacity available in the network to accommodate more DGs. OLTCs have a fixed number of total tap changes available therefore reducing the total daily number of tap operations prolongs the life of OLTC. Reducing network losses increases the utilisation of generation and reduces the impacts on the environment.

3.1 Network losses

Losses are calculated based on the difference between the real power at the sending end and the receiving end. Total network losses for four test cases are plotted in Fig. 3 at half-hour resolution and total network losses in 24 h are calculated in Table 1.

It can be observed that the inclusion of DG can reduce network losses. In scenario 4, by avoiding reverse power flow, network losses can be further reduced. However, the use of reactive power for stabilising voltage increases the network losses in 24 h.

3.2 Voltage

In scenarios 1 and 2, where only OLTCs are used for voltage control, the only voltage at the secondary sides of the transformers is regulated to be close to 1.03 p.u. On the contrary, in scenarios 3 and 4, the new limit of between 0.97 and 1.03 p.u. is applied. Maximum and minimum voltage in the network during 24 h are summarised below in Table 2. It can be seen that DG can increase both the maximum and minimum voltage in the network. Higher maximum voltage means smaller voltage headroom to

Table 2 Maximum and minimum voltage in 24 h

Test case		Maximum voltage, p.u.	Minimum voltage, p.u.
1	no DG	1.040	0.995
2	with DG	1.043	0.996
3	ESS for voltage control	1.030	0.970
4	ESS for power flow management	1.030	0.985

Table 3 Total number of tap changes in 24 h

Test case		Total number of tap changes
1	no DG	106
2	with DG	138
3	ESS for voltage control	138
4	ESS for power flow management	138

accommodate more DGs. When ESSs are used for voltage control and power flow management, it can be seen that the maximum voltage is limited to 1.03 p.u. Lower maximum voltage means that more DGs can be connected to the network.

3.3 Number of tap changes

The total number of OLTC tap changes in 24 h for all 31 transformers is detailed in Table 3. As can be seen, DG increases the total number of tap changes. The ESSs in this study are embedded in the feeders, therefore they are not able to reduce the number of tap changes.

3.4 Power flow

Total power import/export of the whole network for 24 h for all four test cases are depicted in Fig. 4. As can be seen, DG can reduce the total power import of the network. During peak PV generation hours, reverse power flow occurs. However, in scenario 4, where ESSs are used to avoid reverse power flow, exporting can be avoided. Avoiding export excess generation can increase the utilisation of local renewable generation and reduce total losses, as shown in Table 1.

4 Conclusion

An actual distribution network is introduced and modelled in Matpower as part of the inteGRIDy project. A smartgrid architecture with ESSs is designed. ESSs are located next to large distributed generators. To explore the impacts of DG and the benefits of the proposed smartgrid architecture, four test cases have been designed, i.e. no DG, with DG, using ESS for voltage control and using ESS for power flow management. Four indices, total network losses, voltage headroom, total power flow and total number of tap changes have been compared. It is found that DG can reduce total network losses. When ESSs are used to avoid reverse power flow, ESSs can further reduce total network losses. With on OLTC controlling voltage, DG increases the maximum voltage in the network, therefore, reduces voltage headroom. When

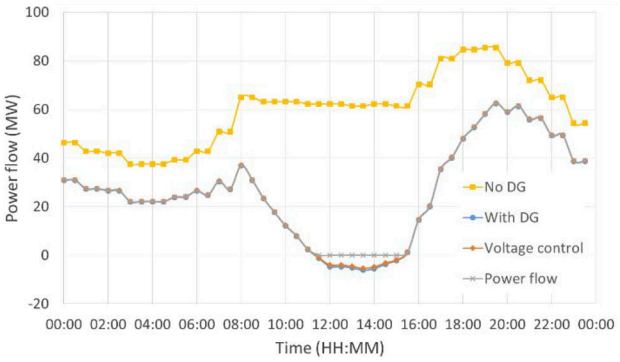

Fig. 4 *Total power import/export*

ESSs are used for voltage control and power flow management, the maximum voltage can be reduced and therefore creates additional voltage headroom. It is also found that compared to the baseline without any DG, DG can increase the total number of tap changes. However, due to the locations and sizes of the ESSs in this study, they are not able to reduce the number of tap changes. Further studies can be carried out to study the use of ESS in reducing tap change operations. In the last study, it has been found that DG can reduce the import of the whole network and during peak PV generation hours, reverse power flow can occur. By charging ESSs during peak PV generation hours and discharge during peak demand period, reverse power flow can be avoided and reduce network losses.

5 Acknowledgments

This paper was presented at the 9th International Conference on Power Electronics, Machines and Drives (PEMD 2018). This work was carried out as part of the inteGRIDy project. The inteGRIDy project is being financed by the European Commission under Grant agreement 731268. The authors also thank Scottish & Southern Electricity Networks for supporting this work.

6 References

[1] Zimmerman, R.D., Murillo-Sanchez, C.E., Thomas, R.J.: 'MATPOWER: steady-state operations, planning, and analysis tools for power systems research and education', *IEEE Trans. Power Syst.*, 2011, **26**, pp. 12–19

[2] 'Long term development statement for southern electricity power distribution PLC's electricity distribution system', Southern Electric Power Distribution, 2016

[3] Lyons, P.F., Wade, N.S., Jiang, T., *et al.*: 'Design and analysis of electrical energy storage demonstration projects on UK distribution networks', *Appl. Energy*, 2015, **137**, pp. 677–691

[4] Wade, N.S., Taylor, P.C., Lang, P.D., *et al.*: 'Evaluating the benefits of an electrical energy storage system in a future smart grid', *Energy Policy*, 2010, **38**, pp. 7180–7188

[5] Tant, J., Geth, F., Six, D., *et al.*: 'Multiobjective battery storage to improve PV integration in residential distribution grids', *IEEE Trans. Sustain. Energy*, 2013, **4**, pp. 182–191

[6] Gabash, A., Li, P.: 'Active-reactive optimal power flow in distribution networks with embedded generation and battery storage', *IEEE Trans. Power Syst.*, 2012, **27**, pp. 2026–2035

[7] Levron, Y., Guerrero, J.M., Beck, Y.: 'Optimal power flow in microgrids with energy storage', *IEEE Trans. Power Syst.*, 2013, **28**, pp. 3226–3234